NGU Report 2006.088

Impact of recent glacial erosion on sub-surface temperatures: the Mid-Norwegian Margin

NGU
Norges geologiske undersøkelse
Geological Survey of Norway

Geological Survey of Norway
NO-7491 Trondheim, Norway
Tel.: 47 73 90 40 11
Telefax 47 73 92 16 20

REPORT

Report no.: 2006.088	ISSN 0800-3416	Grading: Confidential to 01.12.2011

Title:
Impact of recent glacial erosion on subsurface temperatures: the Mid-Norwegian Margin

Authors: Christophe Pascal and Kirsti Midttømme	Client: Pertra ASA
County:	Commune:
Map-sheet name	Number of pages: 25 Price (NOK): Map enclosures:

Fieldwork carried out:	Date of report: 01.12.2006	Project no.: 3154.00	Person responsible:

Summary:

Plio-Pleistocene glaciations lasted for more than 3 Myr in Fennoscandia and were responsible for deep erosion of the mainland and parts of its margin. The amount of erosion on the Mid-Norwegian Margin is estimated to vary from some hundred of meters up to more than one kilometre at the present-day coastline, whereas up to 1000 m of sediments deposited on more distal regions of the margin. Although good constraints are available on the amount of glacio-fluvial material deposited on the margins and the oceanic basins, significant uncertainties on the timing and duration of the sedimentation exist. The uncertainties related to the dating of the Quaternary sediments leave room to different alternatives for the amounts and timing of denudation near shore and onshore and redeposition offshore. In turn, rapid erosion and sedimentation in glacial times has certainly left the regions concerned by these mass redistributions in a disturbed thermal state today.

In order to get a quantitative assessment on the impact of heavy glacial erosion/sedimentation on subsurface temperatures, we conducted 2D finite-element thermal modelling calibrated by heat flow and thermal conductivity measurements. Three different time scenarios were considered: (1) total erosion/sedimentation at t = 2.8Ma, (2) total erosion/sedimentation at t = 0.4 Ma and (3) half erosion/sedimentation at t = 2.8Ma and the other half at t = 0.4 Ma. The modelling suggests that the vigorous glacial action resulted in a strong modification of the thermal state of the Mid-Norwegian Margin. In particular, scenario (2) suggests that the sedimentary basins offshore are still in a transient thermal state.

Keywords: Geofysikk (Geophysics)	Kontinentalsokkel (Continental shelf)	Modellering (Modelling)
Varmestrøm (Heat flow)	Petrofysikk (Petrophysics)	Iserosjon (Glacial erosion)
		Fagrapport (Scientific report)

CONTENTS

1 INTRODUCTION

Plio-Pleistocene glaciations lasted for more than 3 Myr in Fennoscandia and were responsible for deep erosion of the mainland and parts of its margin (Dahlgren et al. 2002). The amount of erosion on the Mid-Norwegian margin is estimated to be some hundred of meters up to more than one kilometer at the present-day coastline whereas up to 1000 m of sediments deposited on more distal regions of the margin (e.g. Riis 1996). Although good constraints are available on the amount of glacio-fluvial material deposited on the margins and the oceanic basins, significant uncertainties on the timing and duration of the sedimentation exist (Rise et al. 2005). This is in particular true for NAUST sequences R and O representing thick packages of glacigenic sediments formed during the very last glacial cycles and whose age is poorly constrained in between 16 and 400 ka BP.

The uncertainties related to the dating of the Quaternary sediments leave room to different alternatives for the amounts and timing of denudation near shore and onshore and redeposition offshore. A scenario that also seems to be supported by geomorphological observations onshore (Lidmar-Bergström et al. 2000) is that much more recent, than previously anticipated, rapid erosion and sedimentation occurred, leaving the regions concerned by these mass redistributions in a disturbed thermal state today.

In summary, it is very unlikely that the traditional thermal steady-state hypothesis (Pollack and Chapman 1977) is applicable to the Norwegian margin. Any attempt to estimate subsurface temperatures (i.e. down to ~5 km depth) has to involve the effect of recent glaciations and, thus, the vigorous capability of glaciers to redistribute masses at the surface.

In order to get a quantitative assessment on the impact of heavy glacial erosion/sedimentation on subsurface temperatures, we conducted finite-element thermal modelling calibrated by heat flow and thermal conductivity measurements. Three "end-member" scenarios for the timing and amount of erosion/sedimentation are modelled here. This short feasibility study represents the first step towards a future and more elaborated research project whose proposal was submitted to the NFR Petromaks Programme in October.

2 HEAT FLOW DATA

2.1 Marine heat flow data

Marine heat flow data have been acquired on the Norwegian margin since the late 60's (Haenel 1974, Langseth and Zielenski 1974, Sundvor et al. 1989, Ritter et al. 2004). Gravity probes equipped with thermistors and with penetration depths down to 4-5 m are routinely used in marine heat flow studies (for a complete description see Haenel 1979). The method presents the advantage of measuring at shallow depths below the sea bed where the geothermal gradient reequibrates very fast and does not contain any signal from long-term changes in surface conditions. The validity of the method has been empirically demonstrated in oceanic basins where clear relationships between heat flow and basement age are seen (e.g. Parsons and Sclater 1977). The use of the method becomes more problematic where the sea floor lies at relatively shallow depths (i.e. less than 1000 m) and is, therefore, influenced by annual to decadal temperature variations of the sea water (see discussion in Ritter et al. 2004).

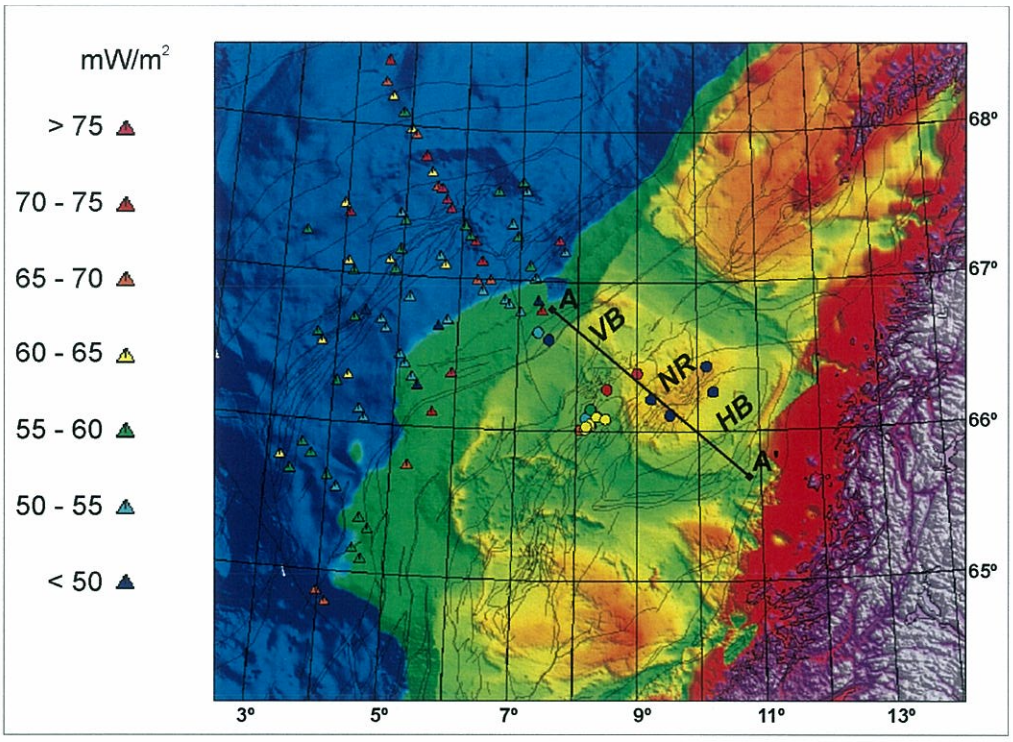

Figure 1. Location map: AA' is the line modelled in this study; heat flow data are represented by triangles (marine heat flow data) and circles (determined from BHT data). See also Fig. 2 and Table 1. VB = Vøring Basin, NR = Nordland Ridge, HG = Helgeland Basin.

A compilation of existing marine heat flow data from the Vøring Margin is shown in Figure 1. Noteworthy, most measurements have been carried out in the Vøring Basin strictu-sensu (i.e. west of Nordland Ridge). The "brutally" averaged heat flow value is ~61 mW/m^2 but its associated standard deviation is as high as ±9 mW/m^2, reflecting significant data dispersion. Furthermore, Figure 2 shows that heat flow values proposed by Sundvor et al. (1989) are usually higher than the ones advanced by Haenel (1974) and Ritter et al. (2004). Although it remains unclear, this systematic bias could be due to differences in procedure or/and equipment used by the different authors. In addition, there is a tendency for higher heat flow values in the outermost part of the Vøring Basin (i.e. where the sedimentary cover thins out but also where the deepest waters prevail, Fig. 2), suggesting lower heat flow where the sedimentary pile is thicker.

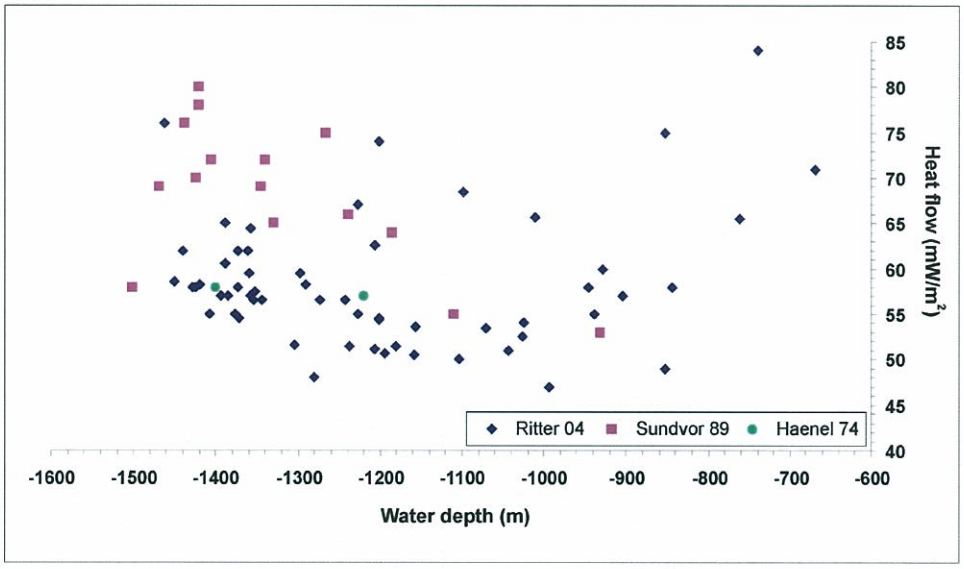

Figure 2. Uncorrected marine heat flow data versus water depth from the Vøring Margin. Note that data for water depths below 1000 m are less reliable.

2.2 Bottom hole temperatures

In the framework of this project we analysed bottom-hole temperatures (BHT) from eighteen wells located less than ~50 km away in a direction perpendicular to the modelled line (Fig. 1). Temperature data are made public by NPD (see www.npd.no). We tentatively estimated heat flow values (Table 1, Fig. 1) from the BHT data using average sea bottom temperatures from Gammelsrød et al. (1992) and thermal conductivities compiled in this study (see chapter 3).

Because NPD does not provide any information on the accuracy of the data and because only one temperature per well is reported, much care has to be taken with the heat flow values calculated here. Nevertheless, it is interesting to note that, on average (i.e. ~60 mW/m^2), these heat flow values remain in reasonable agreement with values previously advanced in the literature (e.g. ~56 mW/m^2 Ritter et al. 2004). The surprisingly high value found for well 6609/7-1 appears to be the consequence of the anomalously high BHT value reported by NPD.

Table 1. Estimated thermal gradients and heat flow from BHT data (see well locations in Figure 1).

drillhole	depth (m)	Deepest formation penetrated	BHT (°C)	Tsurf (°C)	Grad. (°C/km)	HF (mW/m^2)
6607/5-1	3778	Lange (L. K.)	112	3	32	48
6607/5-2	4641	Kvitnos (L. K.)	140	1,5	34	50, 5
6608/8-1	2982	Zechstein (L. Perm.)	132	3,5	48,5	73
6608/10-1	3412	Åre (E. Jura.)	110	3	35	53
6608/10-3	2896	Åre (E. Jura.)	115	3	44,5	67
6608/10-4	2777	Åre (E. Jura.)	103	3	42	63
6608/10-5	3175	Åre (E. Jura.)	116	3,5	40	59,5
6608/10-6	2079	Åre (E. Jura.)	75	3	42	63,5
6608/10-7	2287	Åre (E. Jura.)	84	3	42	63,5
6608/10-8	2626	Åre (E. Jura.)	97	3	42	63
6608/10-8A	2516	Tilje (E. Jura.)	94	3	42,5	64
6608/11-2	2179	Grey Beds (L. Trias)	80	3,5	42	63
6608/11-3	2007	Grey Beds (L. Trias)	72	3	42	63
6609/7-1	1944	Pre-Devonian (siltstone)	125	5	71	106
6609/10-1	2141	Red beds (L. Trias)	64	5	31	47
6609/11-1	3042	Åre (L. Trias)	90	5	30	45,5
6610/7-1	3307	Red beds (L. Trias)	100	5	31	47
6610/7-2	4191	Grey beds (E. Trias)	112	5	27	40,5
Average					40	59,5

3 THERMAL CONDUCTIVITY DATA

3.1 Determination of thermal conductivities

Thermal conductivity of sedimentary rocks is a key parameter in temperature modelling, because it controls the conductive heat flow, one of the main mechanisms of heat transfer in sedimentary basins. The thermal gradient by conduction is described by Fourier's law as inversely proportional to the thermal conductivity for a given heat flow:

$$q = -k \cdot \frac{dT}{dZ} \qquad (1)$$

where q is heat flow (W/m^2), k is thermal conductivity (W/m/K) and dT/dZ represents the temperature gradient.

Table 2 . Thermal conductivities associated to different lithologies.

Lithology	Thermal conductivity W/m/K
Shale and claystone	1.2
Silty claystone	1.4
Siltstone	2.0
Silty /clayey sandstone	3.0
Sandstone	3.5
Limestone	2.0
Volcanic intrusive	2.0
Salt	6.0

There still exists a lack of basic knowledge about the thermal conductivity of sedimentary rocks and, in particular, reliable information concerning claystones and shales is scarce (e.g. Demongodin et al. 1993, Gallagher et al. 1997, Midttømme and Roaldset 1999). Blackwell and Steele (1989) concluded that thermal conductivities of shales were 25 to 50% lower than reported values in the literature and did not appear to vary as a function of compaction in the expected way.

Thermal conductivity is estimated for each formation as a function of lithology. The formation conductivity is calculated using the harmonic mean model:

$$\frac{1}{k} = \sum \frac{Vi}{ki} \qquad (2)$$

where i represents a lithology component, k_i the thermal conductivity associated to i and V_i its volume.

The harmonic mean model, also known as the series flow model, is a mixing law model where the conductivity is calculated from the lithology and the lithology conductivities. By harmonic mean the thermal resistivities of the lithologies (the reciprocals of the conductivities) are added together. This model gives the lower limit of the formation conductivity, while the arithmetic mean model (parallel flow model) gives the upper limit of formation conductivity.

Thermal conductivities values of the lithologies (Table 2) are based on data from the Norwegian shelf (Midttømme 1997), measured conductivities from onshore wells in Denmark (Balling et al. 1981) and values published by Blackwell and Steele (1989).

Thermal conductivity of silty claystone and silty/clayey sandstone is estimated by the geometric mean of the thermal conductivities of claystone, siltstone and sandstone:

$$k = k_{L1}^{VL1} \cdot k_{L2}^{VL2} \qquad (3)$$

where k_{L1} and V_{L1} represent respectively the thermal conductivity and volume of lithology L1.

Table 3. Estimated thermal conductivity of the well formations.

Period	Group	Formation	6607/5-1	6607/5-2	6609/7-1	6509/10-1	6609/11-1	6510/2-1
Pliocene	*Nordland*	*Naust*	**1,4**					
Miocene			**1,3**					
Eocene	*Hordaland*	*Brygge*		**1,2**	**1,4**	**1.8**	**1,3**	
	Rogaland	*Tare*	**1,4**	**1,3**	**1,3**	**1,6**	**1,4**	
		Tang		**1,2**			**1,6**	
U. Cretac	*Shetland*	*Springar*	**1,3**	**1,2**	**1,3**	**1,4**	**1,3**	
		Nise	**1,9**	**1,3**				
		Kvitnos		**1,3**				
L. Cretac		*Crom. Knoll*	**1,4**		**1,5**		**1,4**	**1,2**
		Lange						
U. Juras		*Spekk*					**1,4**	**1,2**
		Melke						
M. Juras	*Fangst*	*Garn*						**1,8**
		Not						**1,3**
		Ile						**1,6**
L. Juras	*Båt*	*Ror*				**1,6**		**1,5**
		Tilje				**3.0**		
		Åre				**1,7**		
U. Trias						**1,7**		**1,6**

Lithological information is based on released well data accessed through the Aceca database. Available wells for this study are 6510/2-1, 6509/10-1, 6609/11-1 6609/7-1, 6607/5-1 and 6607/5-2. Estimated thermal conductivities for the different formations are given in Table 3.

3.2 Further remarks

In this study thermal conductivity is mainly determined from the grain size distribution. For sandstone sequences mineralogy and porosity will affect the thermal conductivity. Data of porosity and mineralogy of the sandstone formations would have improved the estimated conductivities of these formations. Shale and claystone are the dominating lithologies in this profile and the mineralogy seems to be of minor importance for these lithologies (Midttømme 1997). Other textural factors will affect the thermal conductivity. Thermal conductivity of shale is anisotropic. Thermal conductivity measured parallel to the layering can exceed by a factor two the conductivity measured perpendicular to the layering (Midttømme 1997). The thermal conductivity of tilted sequences will therefore have higher thermal conductivity than tabular sequences. In profiles with tilted sequences and/or horizontal variations in lithologies, lateral heat flow transfer can become significant.

4 THERMAL MODELLING

4.1 Introduction and model set up

We used a finite-element technique to compute transient geotherms along the AA' profile, which is a part of the DD' profile from Blystad et al. (1995). The 2D profile was depth converted and slightly reinterpreted by Exploro Geoservices (Fig. 3). The depth-converted geometry was imported in the finite-element code after merging some of the layers that were much too thin to produce significant effects on the final results. This procedure of simplification of the geometry allows for reducing calculation time while keeping the models sufficiently accurate.

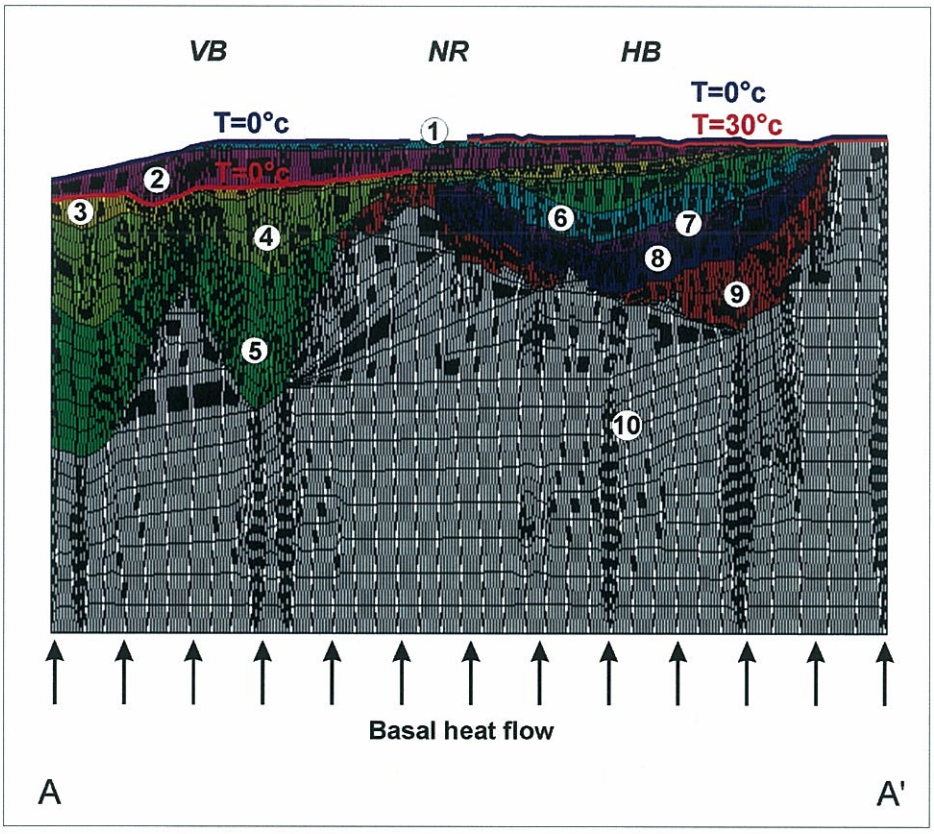

Figure 3. Numerical model mesh and setup. Temperature conditions are changed during modelling runs in order to simulate the thermal effects of sudden erosion in the eastern part of the model and subsequent sedimentation in the western part. Red and blue symbols and numbers depict temperature conditions before and after glacial erosion/sedimentation respectively. Each material symbolised by a specific colour and number was assigned property values given in Table 4. The modelled area is 240 km long and 15 km deep (V.E. * 10). See Fig. 1 for location. VB = Vøring Basin, NR = Nordland Ridge, HG = Helgeland Basin.

The 2D equation of conduction of heat (Carslaw and Jaeger 1959) is used to compute transient geotherms:

$$\frac{\partial^2 T}{\partial x^2} + \frac{\partial^2 T}{\partial z^2} = \frac{\rho c}{k} \frac{\partial T}{\partial t} \qquad (4)$$

where ρ, c and k are respectively density, heat capacity and thermal conductivity.

Imposed boundary conditions are constant heat flow at the model's bottom and varying temperatures at or near its top surface (Fig. 3). The top surface temperatures are varied in order to simulate addition (sedimentation) or removal (erosion) of material by ice action. More precisely, for each modelled scenario a pre-glacial steady-state solution is computed followed by one or two abrupt changes in surface conditions (i.e. erosion/sedimentation is instantaneous in one or two steps). Re-equilibration through time of the disturbed thermal state is then computed according to equation (4).

Table 4. Material parameters used in the modelling (see Fig. 3).

Material		Density* (kg/m^3)	Thermal conductivity ** (W/m/K)	Specific heat (J/kg/K)
1	Quaternary	1900	1,4	1030
2	Pliocene	2100	1,4	-
3	Tertiary	2200	1,5	-
4	Upper Cretaceous	2350	1,3	-
5	Lower Cretaceous	2500	1,4	-
6	Jurassic	2700	1,5	-
7	Trias	2700	1,6	-
8	Trias	2700	1,7	-
9	Permian	2700	2	-
10	Basement	2800	2,5	-

* after NGU's in-house database

** averaged from values in Table 3, inferred values for Permian and basement

4.2 Modelling scenarios

Up to ~1200 m of glaciogenic sediments were deposited in the Vøring Basin along the modelled profile. The amount of material eroded away on land and on the shelf remains a matter of debate. On the mid-Norwegian margin, the Naust Formation accumulated rapidly as a response to the glaciations from 2.8 Ma onwards. The main part of the Plio-Pleistocene erosion was focused on the mainland until about 300-400 ka (Bugge et al., 2004). A fundamental change then occurred, as the sediments on the shelf began to be eroded and older units started to be exhumed. In the present study we assumed that 1000 m of sediments were eroded in an area located in between the coastline and the Nordland Ridge (Fig. 1 and 3). Three different time scenarios were considered: (1) total erosion/sedimentation at t = 2.8Ma,

(2) total erosion/sedimentation at t = 0.4 Ma and (3) half erosion/sedimentation at t = 2.8Ma and the other half at t = 0.4 Ma. In addition, we tested two different values for the basal heat flow (i.e. 40 and 60 mW/m^2).

4.3 Results

4.3.1 Pre-glacial situation

The initial heat flow distributions for basal heat flow values of 40 and 60 mW/m^2 are shown in Figure 4. Despite heat flow values at the base of the models in kept constant along strike, surface and near-surface heat flow values can differ from these imposed basal heat flow values by ±5 mW/m^2. Note that the strong anomalies at the eastern tip of the Nordland Ridge are partly caused by artefacts due to the sharp lateral variations in the imposed boundary temperatures (Fig. 3). These do not affect notably modelling results at greater depths, especially after thermal re-equilibration runs have been carried out. Variation of surface heat flow along strike is the first modelling result from the present study.

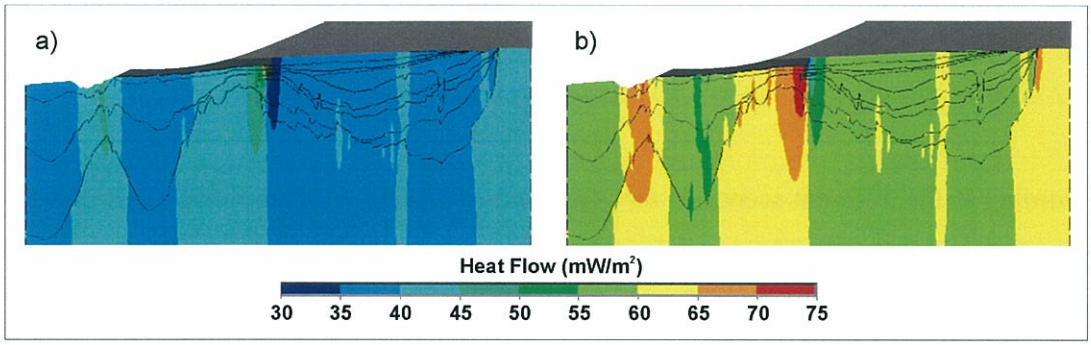

Figure 4. Modelled initial (pre-glacial erosion/sedimentation) vertical heat flow distributions for basal heat flow values of 40 (a) and 60 mW/m^2 (b) respectively.

Figure 5 highlights the cause for these surface heat flow variations. As shown by the distributions of isotherms, the deep sedimentary basins (i.e. Vøring and Helgeland basins) along the modelled profile have a strong blanketing effect on the basement. This effect is due to the fact that sediments present lower thermal conductivities than basement rocks (Table 4). As a result, the warmest basement temperatures are found below the sedimentary basins, implying lateral heat flow towards basement highs (where temperatures are lower for the

same reference level) and increased heat flow at their surface but decreased heat flow on top of the basins.

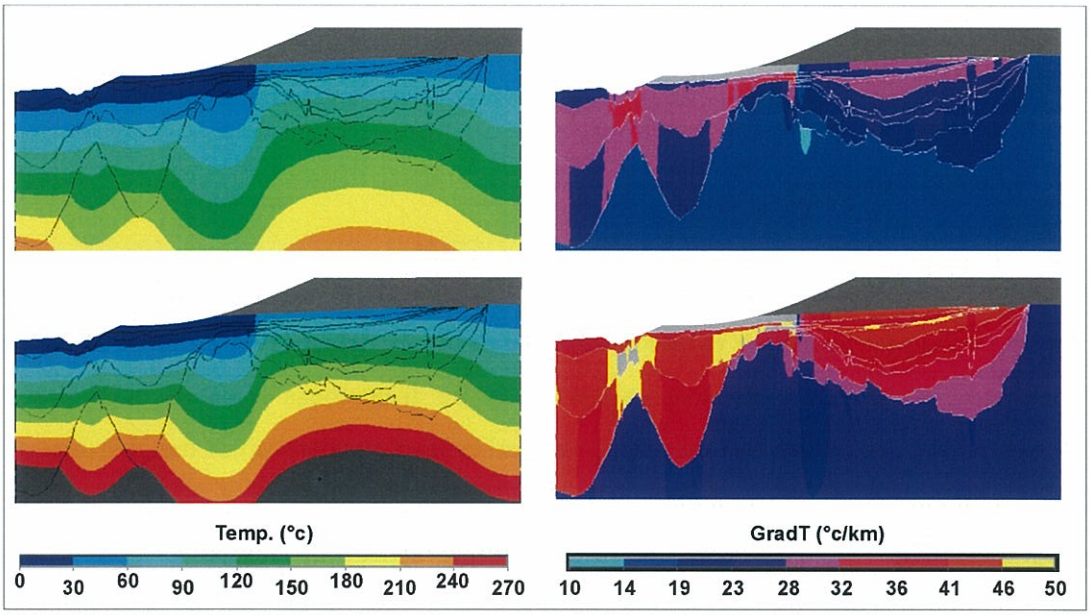

Figure 5 Modelled initial (pre-glacial erosion/sedimentation) thermal configurations for basal heat flow values of 40 (upper row) and 60 mW/m^2 (lower row) respectively.

4.3.2 Glacial forcing of the thermal state and present-day situation

According to the different scenarios for glacial erosion/sedimentation listed in section 4.2 and the two considered cases for basal heat flow values, we carried out six different modelling runs. Predicted isotherms in the range between 60 and 120 °C are depicted in Figures 6 and 7. The modelling shows that the timing for mass redistribution at the surface of the models exerts a strong control on the thermal state at depth. For example, the modelled present-day thermal situation depicted in Figure 6b follows glacial erosion/sedimentation at 2.8 Ma. For this specific case and the temperature window shown in Figures 6 and 7, the present-day thermal state is predicted to have reached a new equilibrium state, where cooling has occurred east of the Nordland Ridge (eroded area) and warming west of it (area of fast sedimentation). This final thermal state differs significantly from the initial thermal configuration (compare Fig. 6a with 6b).

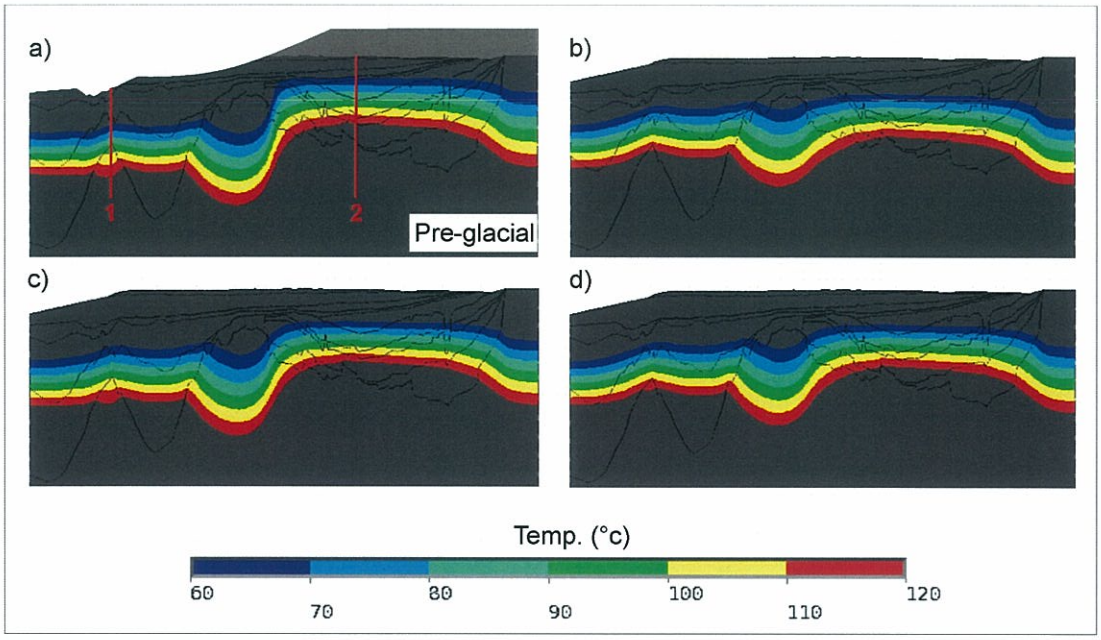

Figure 6. Modelled isotherms for a basal heat flow value of 40 mW/m^2. a) Initial (pre-glacial erosion/sedimentation) situation. b) c) and d) depict present-day situations for erosion/sedimentation having taken place at 2.8 Ma, 0.4 Ma and 2.8 + 0.4 Ma respectively.

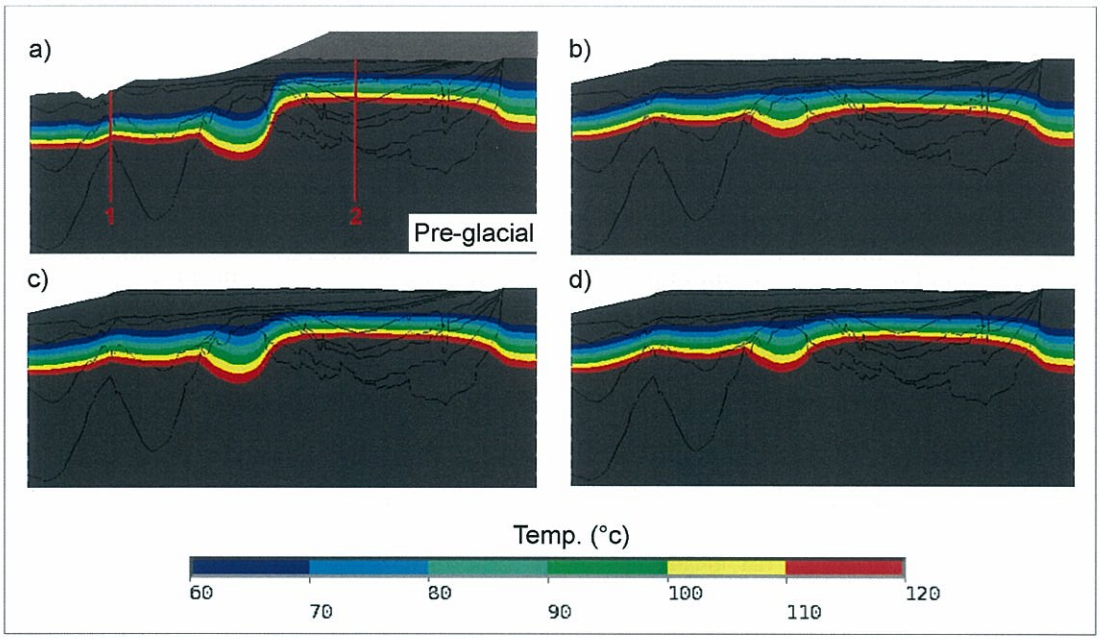

Figure 7. Modelled isotherms for a basal heat flow value of 60 mW/m^2. a) Initial (pre-glacial erosion/sedimentation) situation. b) c) and d) depict present-day situations for erosion/sedimentation having taken place at 2.8 Ma, 0.4 Ma and 2.8 + 0.4 Ma respectively.

In the case where erosion/sedimentation occurred at 0.4 Ma (Fig. 6c), the underground temperatures in between 60 and 120 °C are still in a transient state today and the shape of the isotherms is still mimicking the initial shape (Fig. 6a). The third modelling scenario, where half of the erosion/sedimentation takes place at 2.8 Ma and the other half at 0.4 Ma (Fig. 6d), results in a present-day thermal situation very similar to the one predicted for the first scenario (compare Fig. 6b with 6d). This is because the thermal perturbation inherited from the first erosion/sedimentation event has almost vanished and the magnitude of the second event is relatively modest (i.e. 500 m of erosion and up to 600 m of sedimentation).

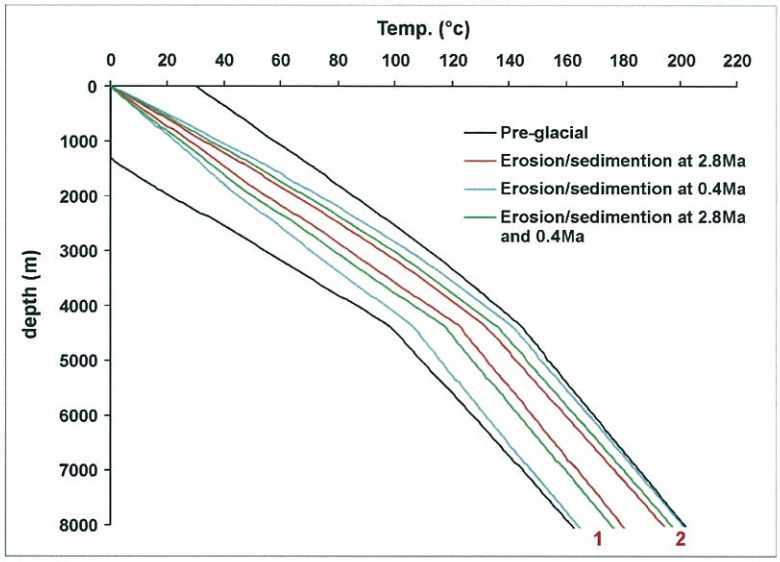

Figure 8. Results from temperature modelling (basal heat flow of 40 mW/m^2): the location of the vertical temperature profiles 1 and 2 is indicated in Fig. 6. Black lines represent pre-glacial erosion/sedimentation geotherms, red, blue and green lines represent present-day geotherms after erosion/sedimentation took place at 2.8 Ma, 0.4 Ma, and half erosion/sedimentation at 2.8 Ma and the other half at 0.4 Ma respectively.

Figures 8 and 9 depict the different modelled geotherms along two vertical profiles. For the three modelled scenarios, the predicted present-day temperatures at depths shallower than ~1000 m have reached or are very close to their final equilibrium state (i.e. red, green and blue geotherms converge for depths < 1000 m). Figures 8 and 9 illustrate clearly the phenomenon of propagation through depth and time of a thermal perturbation having taken place at the upper boundary of the system. For example, consider the blue geotherm along vertical profile 2 showing the present-day situation after erosion at 0.4 Ma (Fig. 8). This geotherm has reached the final thermal equilibrium state at very shallow depths but shows characteristic temperatures of the initial equilibrium state at depths greater than ~7500m (i.e. coincides with the black geotherm). Alternatively, for the green temperature profile, showing

also the present-day situation but with part of the erosion having taken place at 2.8 Ma, the deepest temperatures tend towards the red geotherm. In brief, for this latter modelled case the surface cooling induced by sudden erosion had time enough to propagate at greater depths than for the previous case associated to the blue profile.

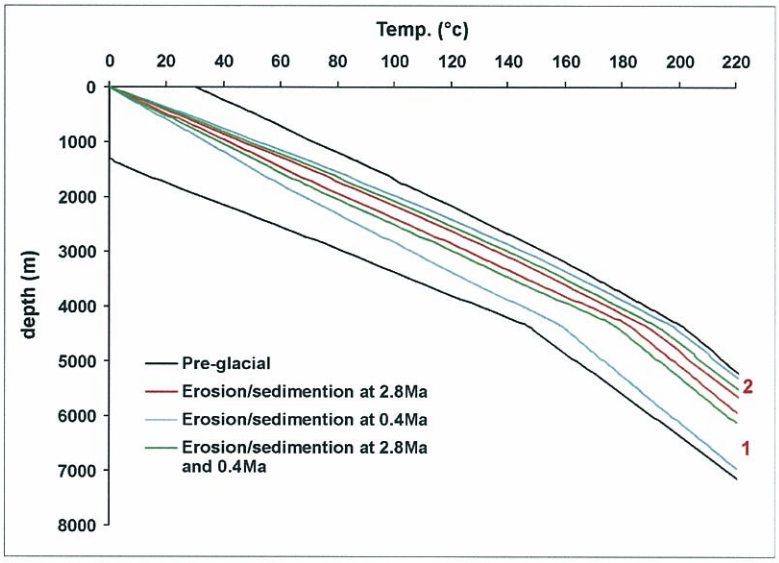

Figure 9. Results from temperature modelling (basal heat flow of 60 mW/m^2): the location of the vertical temperature profiles 1 and 2 is indicated in Fig. 7. Black lines represent pre-glacial erosion/sedimentation geotherms, red, blue and green lines represent present-day geotherms after erosion/sedimentation took place at 2.8 Ma, 0.4 Ma, and half erosion/sedimentation at 2.8 Ma and the other half at 0.4 Ma respectively.

In detail, the predicted maximum decrease in subsurface temperatures due to sudden erosion at 2.8 Ma is 14 to 25 °C for the depth range 1000 to 4000 m (Fig. 8 and 9, black and red profiles 2). This range of temperature drops appears not to be dependent on basal heat flow values. Inside the same depth range, the predicted maximum increase in subsurface temperatures due to sudden sedimentation is 25 to 36 °C and 38 to 54 °C for basal heat flow values of 40 mW/m^2 (Fig. 8) and 60 mW/m^2 (Fig. 9) respectively. Hence, temperature variations depend on the basal heat flow value only in areas where sedimentation took place. This is explained by the blanketing effect due to the low conductivity of the Plio-Pleistocene sediments, which becomes stronger when increasing heat flow.

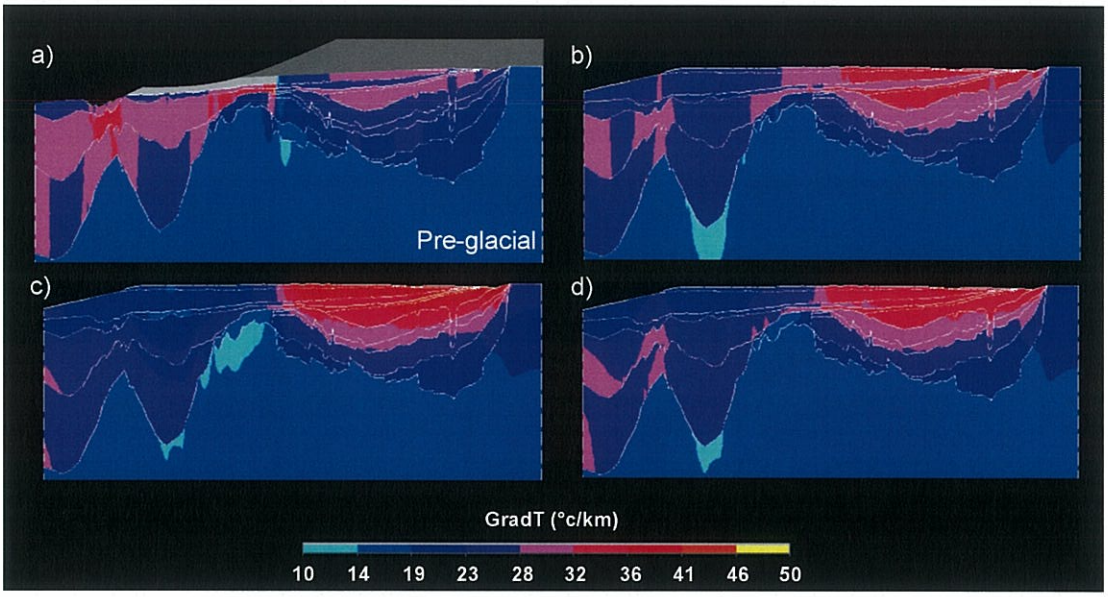

Figure 10. Modelled thermal vertical gradients for a basal heat flow values of 40 mW/m^2. a) Initial (pre-glacial erosion/sedimentation) situation. b) c) and d) depict present-day situations for erosion/sedimentation having taken place at 2.8 Ma, 0.4 Ma and 2.8 + 0.4 Ma respectively.

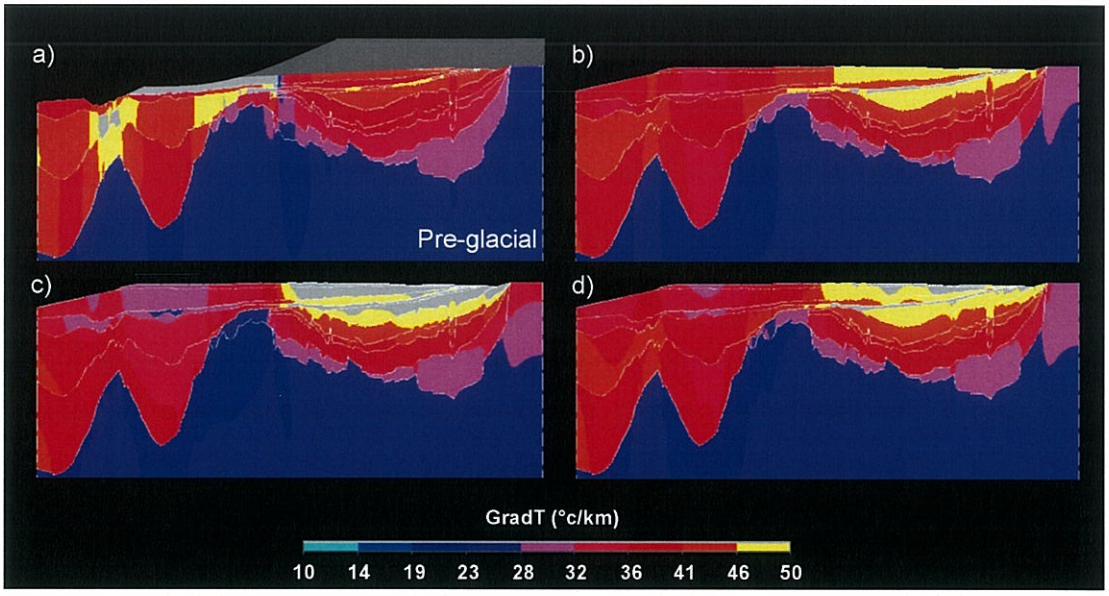

Figure 11. Modelled thermal vertical gradients for a basal heat flow value of 60 mW/m^2. a) Initial (pre-glacial erosion/sedimentation) situation. b) c) and d) depict present-day situations for erosion/sedimentation having taken place at 2.8 Ma, 0.4 Ma and 2.8 + 0.4 Ma respectively.

The resulting present-day thermal gradients for the entire modelled profile is better seen on Figures 10 and 11. As expected thermal gradients increase in areas where sediments have been eroded away but decrease where quick sedimentation has taken place. Note that, for a fixed basal heat flow value, the highest and the lowest gradients in the sedimentary basins are predicted for the modelled case where erosion/sedimentation occurred at 0.4 Ma (Fig. 10c and 11c). Again, these gradients reflect the thermal transient state inherited from a relatively recent perturbation. Finally, it is worth noting that gradient values in the sedimentary basins are predicted to range present-day in between 30 to 40 °C/km for the 40 mW/m^2 cases (Fig. 10) but reach and even exceed 50 °C/km for the 60 mW/m^2 cases (Fig. 11).

5 DISCUSSION

Although the different heat flow determinations used in this study need to be considered with much care (see Chapter 2), they seem to indicate that the present-day heat flow along the modelled line is close to some 60 mW/m^2 on average. Hence, these data would better support models that assume such a value for the basal heat flow (Fig. 4). However, the corresponding modelled present-day thermal gradients appear to be unreasonably high (Fig. 11). In contrast, the models with a basal heat flow of 40 mW/m^2 predict apparently too low surface heat flow values (Fig. 4) but reasonable thermal gradients (Fig. 10 and Table 1). A way to reconcile observed values for heat flow and thermal gradients with our models is to increase the thermal conductivity associated to the sediments. As stated in section 3.2, thermal conductivities were determined on the basis of grain size distributions for sandstone and assuming isotropy for claystone and shales. In the time frame of the present project it has not been possible to conduct further conductivity studies to confirm or reject the values that are proposed in Table 3. Nevertheless, these additional remarks do not affect the validity of the fundamental conclusion from the present modelling study that glacial erosion/sedimentation had a strong influence on the evolution of subsurface temperatures in the Mid-Norwegian margin.

6 CONCLUSIONS AND RECOMMENDATIONS

The present modelling study suggests that temperatures at depths, where petroleum systems are typically found on the Mid-Norwegian margin, were significantly affected by recent glacial erosion/sedimentation. An inescapable conclusion from our modelling study is that the thermal state of the basins present on the Mid-Norwegian Margin has been strongly modified during the past 3 Myr. The thermal state in the sedimentary basins is potentially in a transient state today depending on the timing of the last erosional event. This would imply that the Vøring Basin is still warming up today whereas the Helgeland Basin would be gradually cooling down.

However, more work is needed in order to estimate accurately the respective amplitudes of the thermal signals inherited from the vigorous mass distribution that took place during the last Ice Age.

In particular, future research needs absolutely to involve:

1) a more accurate BHT database with well temperatures recorded at different depths (in order to detect potential transient geotherms);
2) further studies on thermal conductivies (in order to get accurate heat flow determinations);
3) a more precise estimation of the amount of eroded material (e.g. using sonic velocities or/and FT data);
4) a more refined dating of Plio-Pleistocene sedimentary wedges.

7 REFERENCES

Balling, N., Kristiansen, J.I., Breiner, N., Poulsen, K.D., Rasmussen, R. & Saxov, S. 1981. Geothermal measurements and subsurface temperature modelling in Denmark. Geoskrifter, 16.

Blackwell, D.D. & Steele, J.L, 1989. Thermal conductivity of rocks: measurements and significance. In: Naeser, N.D. & McCulloh, T.H (eds) Thermal History of Sedimentary Basins: Methods and Case Histories. Springer-Verlag, New York, 13-36.

Blystad, P. Brekke, H., Færseth, R.B., Larsen, B.T., Skogseid, J. & Tørudbakken, B. 1995: Structural Elements of the Norwegian Continental Shelf. Norwegian Petroleum Directorate Bulletin 8, Part II: The Norwegian Sea Region, 45pp.

Bugge, T., Eidvin, T., Smelror, M., Ayers, S., Ottesen, D., Rise, L., Andersen, E.S., Dahlgren, T., Evans, D. & Henriksen, S. 2004: The Middle and Upper Cenozoic depositional systems on the Mid- Norwegian continental margin.(Abstract) Deep Water Sedimentary Systems of Arctic and North Atlantic Margins, Stavanger, Norway. 276.

Carslaw, H. S., & Jaeger, J. C., 1959. Conduction of heat in solids. Oxford University Press, New York, 510 p.

Dahlgren, K.I., Vorren, T.O., and Laberg, J.S., 2002. Late Quaternary glacial development of the mid-Norwegian margin – 65°-68°N. Marine and Petroleum Geology, 19, 1089-1113.

Demongodin, L., Vasseur, G. & Brigaud, F. 1993: Anisotropy of thermal conductivity in clayey formations. In A.G.Doré et. al. (eds.) Basin Modelling: Advances and Applications. Norwegian Petroleum Society Special Publications. No 3 Elsevier, 209-217.

Gallagher, K. Ramsdal, M., Lonergan, L. & Morrow, D. 1997. The role of thermal conductivity measurements in modelling thermal histories in sedimentary basins. Marine and Petroleum Geology, 14, 201-214.

Gammelsrød, T., Østerhus, S., & Godøy, Ø., 1992. Decadal variations of ocean climate in the Norwegian Sea observed at Ocean Station 'Mike' (66N 02E). ICES Marine Science Symposium, 195, 68-75.

Haenel, R., 1974. Heat flow measurements in the Norwegian Sea. Meteor-Forschungsergebnisse Reihe C: Geologie und Geophysik, 17, 74-78.

Haenel, R. 1979. A critical review of heat flow measurements in Sea and lake bottom sediments. In V. Cermak and L. Rybach (eds.), *Terrestrial heat flow in Europe,* p. 49-73, Springer-Verlag, Berlin.

Langseth, M.G., & Zielinski, G.W., 1974. Marine heat flow measurements in the Norwegian-Greenland Sea and in the vicinity of Iceland. NATO ASI Series. Series C: Mathematical and Physical Sciences. 11; Geodynamics of Iceland and the North Atlantic area, 277-295.

Lidmar-Bergström, K., Ollier, C.D., and Sulebak, J.R., 2000. Landforms and uplift history of Southern Norway. Global and Planetary Change, 24, 211-231.

Midttømme, K. 1997. Thermal conductivity of sedimentary rocks – selected methodological mineralogical and textural studies. Dr.ing. thesis, NTNU 1997:142.

Midttømme, K & Roaldset, E. 1999. Thermal conductivity of sedimentary rocks: uncertainties in measurements and modelling. In: A.C. Aplin A.J.Fleet & J.H.S. Macquaker (eds), Muds and Mudstones: Physical and Fluid Flow Properties. Geological Society, London, Special Publications, 158, 45-60.

Parsons, B., and Sclater, J.G., 1977. An analysis of the variation of ocean floor bathymetry and heat flow with age. J. Geophys. Res., 82, 803-827.

Pollack, H.N., and Chapman, D.S., 1977. On the regional variation of heat flow, geotherms, and lithospheric thickness. Tectonophysics, 38, 279-296.

Riis, F., 1996. Quantification of Cenozoic vertical movements of Scandinavia by correlation of morphological surfaces with offshore data. Global and Planetary Change, 12, 331-357.

Rise, L., Ottesen, D., Berg, K., and Lundin, E., 2005. Large-scale development of the mid-Norwegian margin during the last 3 million years. Marine and Petroleum Geology, 22, 33-44.

Ritter, U., Zielinski, G.W., Weiss, H.M., Zielinski, R.L.B. & Sættem, J. 2004: Heat flow in the Vøring Basin, Mid. Norwegian Shelf. Petroleum Geoscience, 10, 353-365.

Sundvor, E., Myrhe, A.M., & Eldholm, O., 1989: Heat flow measurements on the Norwegian continental margin during the Flunorge project. Univ. of Bergen Seismo Series, 27.